

# Coastal vulnerability assessment: through regional to local downscaling of wave characteristics along the bay of Lalzit (Albania)

Francesco De Leo<sup>1</sup>, Giovanni Besio<sup>1</sup>, Guido Zolezzi<sup>2</sup>, and Marco Bezzi<sup>2</sup>

<sup>1</sup>Dept. of Civil, Chemical and Environmental Engineering - University of Genoa, Genoa, 16145, Italy

<sup>2</sup>UNESCO Chair in Engineering for Human and Sustainable Development - Dept. of Civil, Environmental and Mechanical Engineering - University of Trento, Trento, 38123, Italy

*Correspondence to:* Francesco De Leo (francesco.deleo@edu.unige.it)

## Abstract.

Coastal vulnerability is evaluated against inundation risk triggered by waves run-up, through the evaluation of vulnerability levels (referred to as “VL”) introduced by Bosom and Jiménez (2011). VL are assessed through different wave climate characterizations, referring to regional (offshore wave climate) or local (near-shore wave climate) scale. The study is set along the Lalzit bay, a coastal area nearby Durrës (Albania). The analysis reveals that the results vary due to uncertainties inherent in the run-up estimation, showing that the computational procedure should be developed by taking into account detailed information about the local wave climate. Different approaches in choosing wave characteristics for run-up estimation affect significantly the estimate of shoreline vulnerability. The analysis also shows the feasibility and challenges of applying VL estimates in contexts characterized by limited data availability, through targeted field measurements of the coast geomorphology and an overall understanding of the recent coastal dynamics and related controlling factors.

## 1 Introduction

Coastal zones are often characterized by a fragile equilibrium, being subjected to hydro-geomorphic processes that change their shape over time and space, and are as well under stress due to the presence of conflicting human activities (Kamphuis, 2010). Moreover, these areas have a huge socio-economic value, which has often triggered their high exploitation in the last decades: coastal population is constantly increasing, together with maritime commerce and coastal tourism (Neumann et al., 2015). This implies enhanced anthropogenic pressures, which challenge their sustainable management and preservation.

The present paper focuses on extreme natural storm events and on their impact on coastal vulnerability within such complex framework. As clearly specified by the Integrated Protocol on Coastal Zone Management (“ICZM”), the effect of storms should be embedded into coastal zone territorial plans and policies, yielding coastal vulnerability assessment (UNEP, 2008). Efficient assessment and decision support tools are required, providing easily accessible information for decision-makers. Coastal vulnerability assessment represents a viable option, because it is helpful to classify the shorelines in relation to their vulnerability towards extreme events, such as storms induced inundation and erosion.

This usually requires to take into account the long term wave statistics and the geomorphology of the beaches to evaluate the level of risk they are exposed to. The estimate of the environmental risk, coupled with the evaluation of the existing anthropic

pressure (economic and industrial activities) leads to vulnerability maps. Different approaches to compute coastal vulnerability have been so far proposed, which differently combine environmental and socio-economic relevant variables (Gornitz et al., 1994; Soukissian et al., 2010; Di Paola et al., 2014; Fitton et al., 2016; Satta et al., 2016; Ciccarelli et al., 2017; Ferreira et al., 2017; Ferreira Silva et al., 2017; Montreuil et al., 2017; Narra et al., 2017; Mavromatidi et al., 2018, among others). A methodological issue of particular concern is related to the computation of wave climate characteristics suitable for estimating vulnerability levels that are of management significance. This can be illustrated by referring to the practical procedure proposed by Bosom and Jiménez (2011) to assess coastal vulnerability to inundation. The procedure foresees to compute the long term run-up values, starting from the ones evaluated through the model of Stockdon et al. (2006) (hereinafter referred to as S2006), and then combining it with the berm or dune heights of a shore to achieve its run-up vulnerability. However, S2006 formulation intrinsically leads to a conservative result, as it quantifies the run-up exceeded by 2% of the total run-up values induced during a given sea state; this means that, for given wave and beach characteristics, the computed run-up is not the one most likely occurring, but one of the highest possibly observed within a hypothetical series of records. Conversely, if the input wave parameters are provided in the near-shore region at a depth of 10m, S2006 has shown to provide estimates closer to a sea state run-up *expected value* (Sancho-García et al., 2012), also in case of an extreme event (Di Risio et al., 2017). This applies a fortiori when the geometry of the study site is complex (as in the case of the Lalzit bay), thus the wave transformation processes become relevant (Plant and Stockdon, 2015). Such an approach requires therefore to change the scale of the wave climate characterization moving from a national/regional scale to a more detailed local scale.

The main goal of the present paper is to quantify differences in assessing coastal vulnerability to inundation when using a regional rather than a local (near-shore) characterization of the wave climate. The study refers to the bay of Lalzit, immediately north of the city of Durrës (Albania, see Fig. 1). The focus on such rapidly developing context also allows to discuss the potential implications of coastal vulnerability assessment when decision-making requires to be highly adaptive and when data availability is scarce. Preliminary studies on the wave climate characterized its directional frames. Building this information, it has been possible to compute new vulnerability levels to be then compared with the offshore omni-directional ones. Such an approach is particularly relevant because it could highlight the critical issues related to coastal zone management when the littoral use and exploitation change drastically between different seasons, and represents an additional novelty of the present work.

VL assessment was performed referring both to offshore and near-shore wave data, to evaluate variations in shoreline vulnerability depending on the employed spatial (regional/local) and temporal scale (extreme events/seasonal/directional).

The paper is organized as follows: in Sect. 2 we present the indexes computation procedure, along with the investigation area and the data used; in Sect. 3 we show results of coastal vulnerability using wave dataset at regional and near-shore scales; in Sect. 4, results are presented and possible future developments and improvements are discussed.

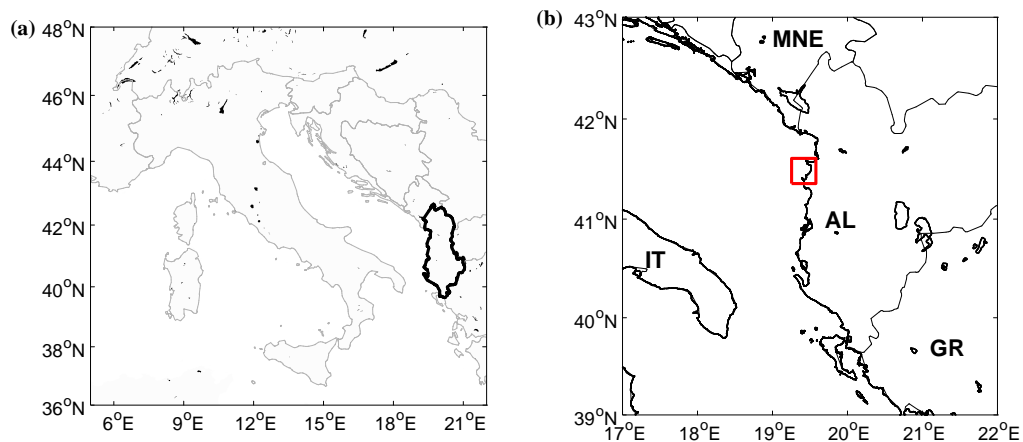


**Figure 1.** Map showing the area under investigation. a) Location of Albania in South-East Europe and b) the bay of Lalzit underlined within the red frame

## 2 Data & Methods

The vulnerability assessment is part of a wider research project, aimed at evaluating and quantifying the ongoing coastal erosion affecting the Lalzit bay area. In order to collect all the required data, a two weeks field campaign was performed during the month of July 2015.

### 5 2.1 Study area: Lalzit bay, Albania

The Lalzit bay is included between two capes, and can therefore be considered as an independent physiographic unit; it is possible to focus on the processes affecting this coastline independently from those characterizing the nearby physiographic units. A physiographic unit is indeed defined as a portion of shoreline with coherent characteristics in terms of natural coastal processes and of land use, which can thus be studied independently from neighbouring shores (UNEP, 2008).

### 10 2.2 Field measurements

Field activities were aimed at collecting the minimum required data to investigate the relevant processes affecting the local coastal dynamics. The geomorphology of the beaches along the bay was characterized through sixteen sections crossing the shoreline, nearly spaced every kilometre along almost twenty km of the bay length (from sec -4, south, to sec 11, north, see Fig. 3a). We recorded the cross-shore section elevation at topographically relevant locations, in correspondence of the main slope changes, with particular attention to the submerged bar system. This allowed to assess the cross-shore sections shape, their berm height and the overall cross-shore profile mean slope (e.g. Fig. 2). Moreover, we collected different sand samples along every section to characterize their grain size distribution. Sediment samples were taken at selected locations along each section. Every sand sample was analysed through a multi-filter sieve, to assess the weight percentages of sand in each size class, thus building the grading curve. The obtained data were then post-processed by using the software Gradistat (Blott and Pye, 2001),

further evaluating the median grain size ( $d_{50}$ ) for every sampled location. As the resulting values of  $d_{50}$  were not significantly varying along each cross-shore profile, we chose to use those characterizing the water edge foreshore as the representative ones of each section.

Results of the grain size surveys are summarized in Fig. 3. The mean grain size ( $d_{50}$ ) happens to be quite homogeneous among all the sections (Fig. 3b), and the granulometry of the bay can be considered representative of a “medium sand”, according to the classification of Wentworth (1922). The only exception is represented by the section next to the Rodoni cape, which is close to a rocky promontory and is therefore characterized by coarser sediments. On the other hand, cross-shore mean slopes ( $\beta_f$ ) and berm heights ( $B_h$ ) are more variable along the coast, with steeper sections being characterized by lower berms and vice-versa (Fig. 3c, d).

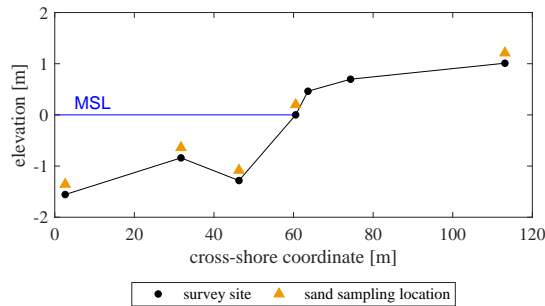


**Figure 2.** Typical cross-shore profile along the Lazlit bay (example of section 2, see Fig. 3a). It is possible to note the presence of the submerged bar some tens of meters away from the coastline

### 10 2.3 Vulnerability levels assessment (VL)

Run-up vulnerability levels are meant to quantify the vulnerability of a coast toward extreme inundation events. VL assessment follows the approach proposed by Bosom and Jiménez (2011): for the investigated beach section (or length of shore), a long term statistical computation for the run-up is required, leading to an intermediate dimensionless variable IV (“Inundation Vulnerability”), defined as follows:

$$15 \quad IV = \frac{Ru_{2\%}}{B_h} \quad (1)$$

where  $B_h$  and  $Ru_{2\%}$  are the beach berm or dune height and the long term run-up respectively. For each section, the IV value is then evaluated within a given range, obtained by setting two boundary values:

$$\begin{cases} IV_{min} = \frac{Ru_{2\%}}{2Ru_{2\%}} & \Rightarrow Ru_{2\%} = 0.5 B_h \\ IV_{max} = \frac{Ru_{2\%}}{Ru_{2\%} - 2} & \Rightarrow Ru_{2\%} = 2 + B_h \end{cases} \quad (2)$$

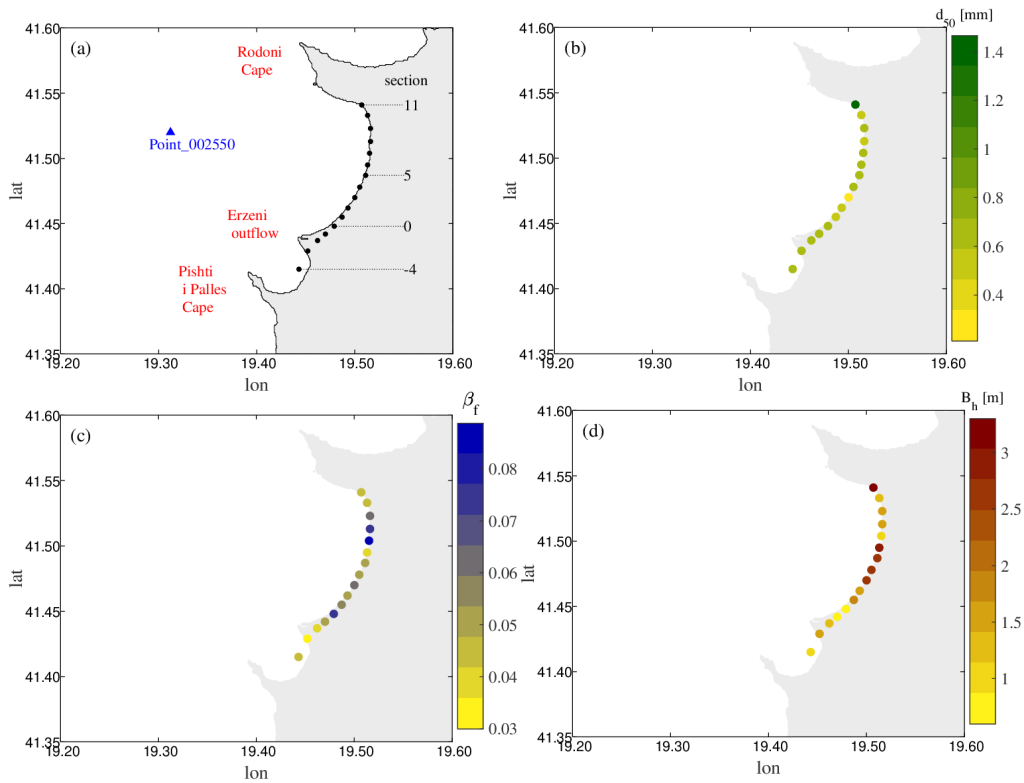


**Figure 3.** a) Sampling locations for beach sections (from -4 to 11, from south to north), Point\_002550 represents DICCA wave hindcast. Spatially distributed values of: b) Median grain size ( $d_{50}$ ); c) Cross-shore mean slope ( $\beta_f$ ); d) Berm height ( $B_h$ )

It can be noticed that the minimum and the maximum values of IV have a clear physical meaning: actually,  $IV_{min}$  is explanatory of the case where the run-up is half of the berm height, ensuring the beach would not be overtopped and thus guaranteeing the protection of the hinterland. On the other hand,  $IV_{max}$  refers to a situation characterized by a run-up two meters higher than the berm height and therefore potentially able to flood the hinterland over a substantial area.

- 5 This interval is then scaled to a range from 0 to 1, grouped in five classes of equally spaced vulnerability levels (“very low”, “low”, “medium”, “high”, “very high”) as reported in Table 1.

IV	0 - 0.2	0.2 - 0.4	0.4 - 0.6	0.6 - 0.8	0.8 - 1.0
VL	very low	low	medium	high	very high

**Table 1.** Vulnerability levels assessment due to the IV variable

## 2.4 Wave data and run-up

The assessment of VL first requires to compute the long term run-up statistics. Regardless the reference model, run-up computation always implies to combine informations about both characteristic wave climate and morphology of a shore (Battjes, 1971; Holman, 1986; Mase, 1989, among others). As regards the wave data, we referred to the hindcast provided by the Department of Civil, Chemical and Environmental Engineering of the University of Genoa ("DICCA", [dicca.unige.it/meteocean/hindcast](http://dicca.unige.it/meteocean/hindcast)). The hindcast is defined all over the Mediterranean sea from 1979 to 2016 with a  $0.1^\circ$  resolution both in longitude and latitude, one hourly sampled, and it is based on NCEP Climate Forecast System Reanalysis ("CFSR"), for the period from January 1979 to December 2010 and CFSv2 for the period from January 2011 to December 2016 (Mentaschi et al., 2013). The DICCA hindcast was widely validated (Mentaschi et al., 2015), and, being densely defined over a large time period, it helps to perform reliable long-term statistical computations (Coles and Pericchi, 2003). The location we referred to for this study is shown in Fig. 3a) (Point\_002550), whereas data about the shore geomorphology were collected as explained in Sect. 2.2.

Run-up is therefore computed according to S2006 as follows:

$$Ru_{2\%} = 1.1 \left\{ 0.35 \beta_f \sqrt{H_0 L_0} + \frac{\left[ H_0 L_0 \left( 0.563 \beta_f^2 + 0.004 \right) \right]^{0.5}}{2} \right\} \quad (3)$$

where  $\beta_f$  stands for the mean slope of the beach,  $H_0$  and  $L_0$  refer to deep water wave height and length respectively.

## 2.5 Extreme Value Analysis (EVA)

When dealing with run-up estimation, if the data linked to the shore characteristics can be well defined, more uncertainties grow up when trying to empirically parametrize exceptional phenomena (extreme events), of which run-up can be considered as an instance. For this reason we tested two different approaches for the estimation of extreme run-up values.

First, in the frame of a regional analysis, we considered the deep-water data as defined in Point\_002550, selecting the annual maxima sea storms from the wave dataset and evaluating the annual maxima run-ups through Eq. (3). This resulted in a 38 extreme run-up dataset for each of the sixteen sections. Every dataset was then modelled through a GEV distribution (Coles et al., 2001), in order to carry out the long term design of run-up values. Given the distributions, we set two target return periods, literally 50yr and 500yr, and further computed the resulting run-ups for every section in both cases. This allowed to quantify how VL estimation could be affected by differently conservative approaches.

Afterwards, we switched from a regional to a locale scale: in this case, EVA were performed directly over the extreme sea storms wave parameters, to assess the 50yr and the 500yr waves. We thus propagated the target waves in front of each section, computing afterwards the long term run-up values. Here, as the wave climate shows different patterns with respect to the average incident waves direction, we split the initial wave dataset according to two meaningful directional fetches. This

choice involved an important consequence: when performing the directional analysis, referring return periods for each of the identified sectors have in fact to be carefully assigned (Forristall, 2004):

$$\begin{cases} F_o = \prod_1^{N_p} F_i \\ F = 1 - \frac{1}{T_R} \end{cases} \quad (4)$$

being  $F$  the probability of non exceedance,  $T_R$  the significant return period and  $N_p$  the number of directional patterns; 5 subscripts  $o$  and  $i$  stand for omnidirectional and the  $i$ -<sup>th</sup> directional pattern, respectively. The  $F_i$  probabilities are fixed in order to obtain  $N_p$  equal values whose product gives  $F_o$  (given the referring omni-directional return period). Then, probabilities obtained with Eq. (4) were retained to carry out the long term significant wave heights, as previously explained for the design run-up values for the regional analysis. In both the cases, the validity of the distribution was tested through the Kolmogorov-Smirnov test (Massey Jr, 1951).

10 To completely characterize the target waves (to be downscaled at a later time in the near-shore zone), we linked the peak periods to the computed long term significant wave heights following the empirical model proposed by Callaghan et al. (2008). As regards the waves mean incident directions, they were assessed due to the particular waves climate of the area. Resulting wave features were therefore propagated over the local bathymetry to get the parameters at a depth of ten meters in front of each of the investigated sections; downscaling of waves was performed through SWAN, a third generation wave model developed 15 to compute waves in coastal regions with shallow waters (Booij et al., 2003). The obtained wave parameters were then used to compute the 10m depth run-up for both the considered return periods. As regards the bathymetry of the bay, we referred both to the ETOPO1 dataset ([www.ngdc.noaa.gov](http://www.ngdc.noaa.gov)) and a nautical chart of the Italian Hydrographic Institute ([www.marina.difesa.it](http://www.marina.difesa.it)).

It is worth mentioning that the return period of a forcing variate is not necessarily equal to the return period of the outcomes. As an instance, a given return period wave may not lead to the corresponding return period run-up (Hawkes et al., 2002, , in 20 this case it depends on the characteristics of the wave climate of the study site). Nevertheless, when performing the regional analysis, the run-up long term curves computed starting from the annual maxima  $H_s$  (say "AM1" approach) happened to lye very close to those linked to the annual maxima retained from the computed initial distribution of run-ups. Furthermore, previous studies demonstrated that this approach can still lead to satisfactory results (Garrity et al., 2007), and it has already been adopted within similar works (Vitousek et al., 2008). We therefore decided to refer to the AM1 approach both for the 25 regional and the local scale (omni-directional and directional analysis respectively), as in the latter case it allows to considerably reduce the computational time and effort (there is no need to downscale the whole wave dataset in the shallow waters, but just the target waves).

### 3 Results

Once we computed the long term run-ups, we evaluated the resulting VL according to the morphology of the testing locations. Since results are punctual (e.g. one index for each of the sixteen sampling locations), we linearly interpolated the VL values within hypothetical intermediate sections, in order to get a more meaningful overview about the whole bay.

- 5 We initially referred to the regional scale; in this case, an omnidirectional analysis was performed, leading to two sets of results linked to the tested return periods. Secondly, we detailed our study to the local scale: in this case, we got two sets of results for every directional sector taken into account. We first present the VL obtained from the regional study.

#### 3.1 Regional scale (offshore wave conditions)

At the regional scale the environmental inputs were the same for each section, being the wave characteristics defined in deep  
10 water (Point\_002550, Fig. 3a); the differences in the run-up significant values were just due to different morphological characteristics of each cross-shore section (literally, the mean slope of the different beach profiles). This can be clearly noticed in Fig. 4: the empirical run-ups show the same distribution for every section, as their values are just rigidly translated of a quantity that depends on the value of the section slope  $\beta_f$  (see Eq. 3). From the curves in Fig. 4, the run-ups linked to 50 and 500yr return period were extrapolated, and the inundation vulnerability levels were accordingly computed, as explained in section  
15 2.3. Results are shown in Fig. 5.

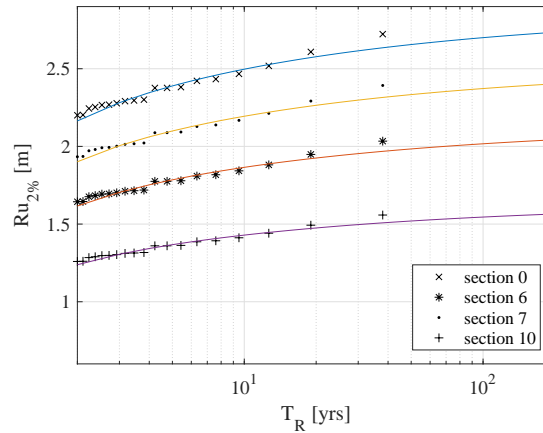


**Figure 4.** Return period curves for the run-up parameter; results are presented for just some of the cross-sections for the sake of clarity



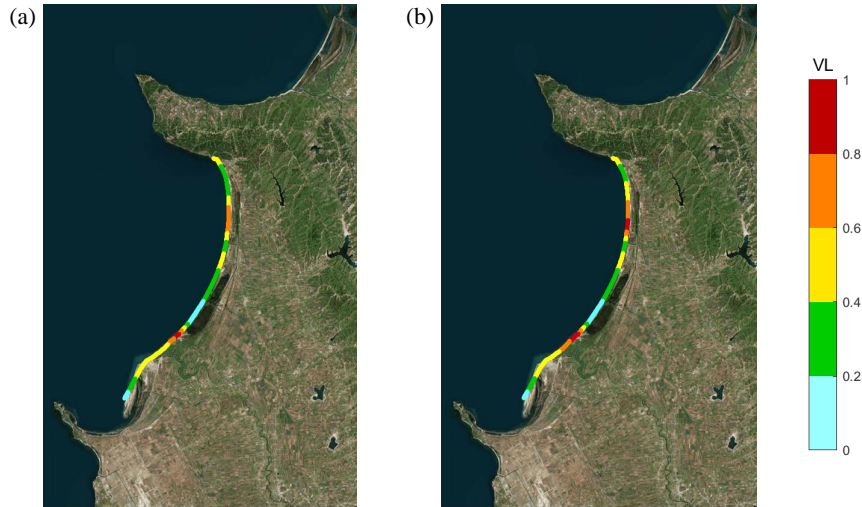


**Figure 5.** Run-up vulnerability levels for the Lalzit bay from the regional analysis, using deep water data: a) 50yr return period; b) 500yr return period

### 3.2 Local scale (nearshore wave conditions)

Evaluation of coastal vulnerability levels has been carried out also by employing the propagated values of the wave climate at the local scale. It has to be remarked that, in this case, the mean cross-shore slope is not the only changing parameter between one section and another: as waves are propagated toward the shore in front of each of the investigated locations, they are modified due to the occurring transformation processes, resulting in different wave characteristics (heights, lengths and incident directions) depending on the position of a section along the bay.

The first step to compute VL at a local scale is to characterize the wave climate. As shown in Fig. 6a), the bay is characterized by waves prevalently propagating from the S-SW and W-NW directions. We therefore considered two directional sectors, literally the third ( $180-270^\circ\text{N}$ , called  $1^{st}$  sector) and fourth ( $270-360^\circ\text{N}$ , called  $2^{nd}$  sector) quadrant of the wave rose. Furthermore, it has been previously shown as the waves incoming direction is tied to the seasonality of the wave climate (De Leo et al., 2017), with S-SW being the prevalent incoming direction for waves generated during winter and autumn. This is still reflecting on the annual maxima wave heights, with those belonging to the second sector more uniformly distributed along the year (even though with the peak of occurrence still happening during winter, see Fig. 6b).

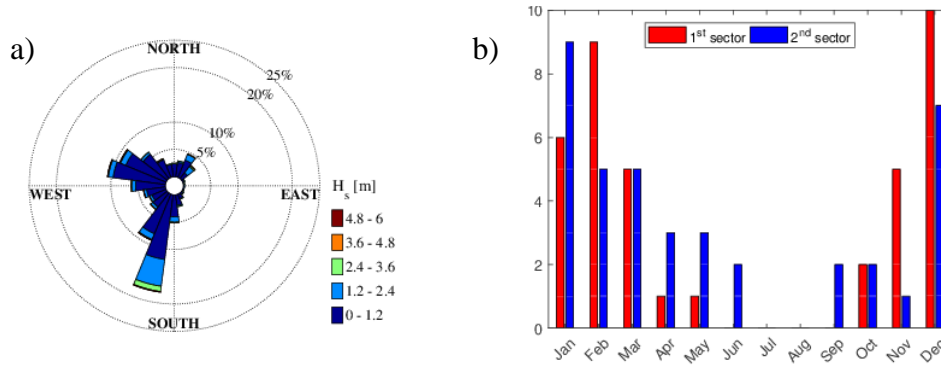


**Figure 6.** a) Rose of significant wave height for hindcast Point\_002550; b) seasonal distribution of the annual maxima wave height due to the considered sectors

Extreme events have been defined for each of the identified sectors, computing the resulting 50yr and 500yr return period wave heights. The target wave incoming direction for each sector was defined through a linear interpolation, in order to minimize the root mean square error with respect to the directions of the AM sea storms (see Fig. 7). Finally, for the wave periods, we evaluated their expected values thanks to the empirical equation of Callaghan et al. (2008) (Eq. 5). This equation was developed assuming a  $H_s/T_p$  conditioned log-normal distribution, which is the most diffused model for these bivariate analysis (see as an instance Haver, 1985; Mathisen and Bitner-Gregersen, 1990, among others). We fit Eq. (5) to the sea storms of the directional sectors, selected through a partial duration series approach fixing a wave height threshold equal to the 98% quantile of the total  $H_s$  and an inter-event duration of 24hrs (details on the PDS approach can be found in Lang et al., 1999; Claps and Laio, 2003).

$$10 \quad \begin{cases} E(T_p) = aH^b + cfH^{d+g} \\ a_1 = 4.3819; b_1 = 0.4134; c_1 = 0.6815; d_1 = 0.0766; f_1 = 0.9875; g_1 = 0.3368 \\ a_2 = 5.0359; b_2 = 0.4252; c_2 = 3.8330; d_2 = -1.8605; f_2 = 3.1491; g_2 = -1.6310 \end{cases} \quad (5)$$

where  $H$  is the target wave height computed through the EVA as previously explained;  $a$ ,  $b$ ,  $c$ ,  $f$ ,  $d$  and  $g$  are the estimated coefficients for the first (subscript 1) and the second (subscript 2) directional sector.

We therefore characterized the design wave for each of the identified directional sectors (W-NW and S-SW), defining its significant height, peak period and angle of attack. These parameters were set at a time as inputs of the wave propagation model, computing the shallow water waves. The starting values are shown in Table 2. The inundation vulnerability levels following the downscaled wave features are shown in Fig. 8 and 9.

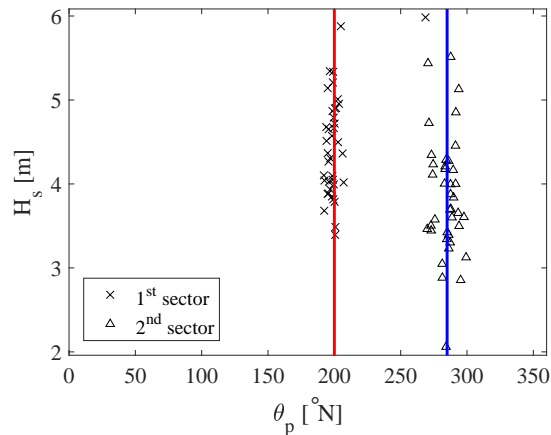


**Figure 7.** Directions of the extremes waves belonging to the two considered sectors

sector	$T_R$ [yrs]	$H_s$ [m]	$T_p$ [s]	$\theta_p$ [°N]
1 <sup>st</sup>	50	6.3	10.8	200.3
	500	7.0	11.3	200.3
2 <sup>nd</sup>	50	5.6	10.5	284.8
	500	6.0	10.8	284.8

**Table 2.** Design wave parameters for the directional sectors. Notations  $T_R$  is the return period,  $H_s$ ,  $T_p$ , and  $\theta_p$  stand for wave height, period and incoming direction, respectively

For the sake of clarity, in order to compare the results obtained with the two different approaches mentioned before, we discuss just the results linked to the punctual investigated sections; analogous considerations can be therefore extended to the intermediate sections, whose vulnerability levels were assessed through a linear interpolation as previously explained.

Looking at the punctual results (Fig. 10 and 11), it can be noticed that in all considered cases even sections lying next to each other can show very different vulnerability levels: as the sampling locations are 1km distant one from another, their morphological characteristics can significantly vary, and this is consequently reflected in the results.

Referring to the regional scale-offshore analysis and 50yr return period, the vulnerability towards inundation happens to be “very high” in section 0, and still “high” in sections 7, 8; sections -4, 1, 2 are characterized by a “very low” vulnerability, whereas sections 3, 4, 6, 9 and 10 show “low” vulnerability; the other ones are characterized by a “medium” vulnerability. As we could expect, vulnerability levels increase when referring to 500yr return period: in this case, a “very high” vulnerability characterizes section 7 as well, whereas the level increase from “medium” to “high” in section -1, and from “low” to “medium” in section 9; vulnerability class does not change for sections -4, -3, -2, and for sections between 0 and 6.

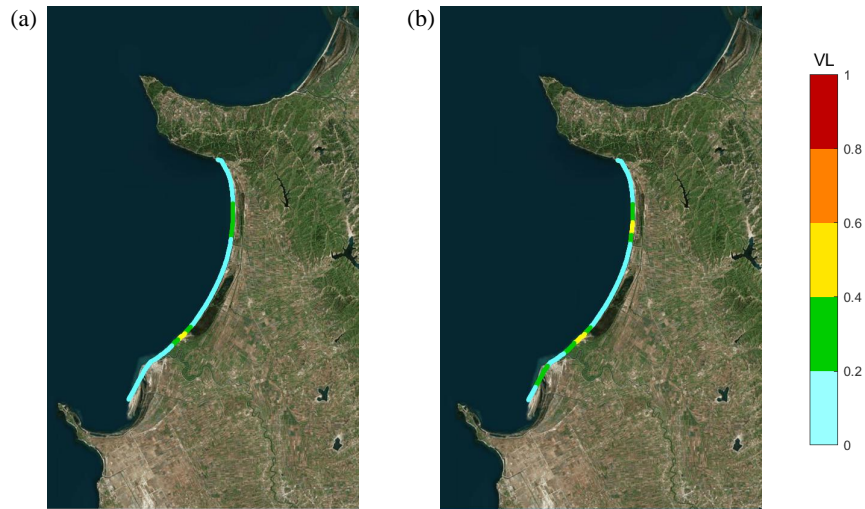


**Figure 8.** Run-up vulnerability levels for the Lalzit bay, using near-shore data for the 180-270°N sector: a) 50yr return period; b) 500yr return period

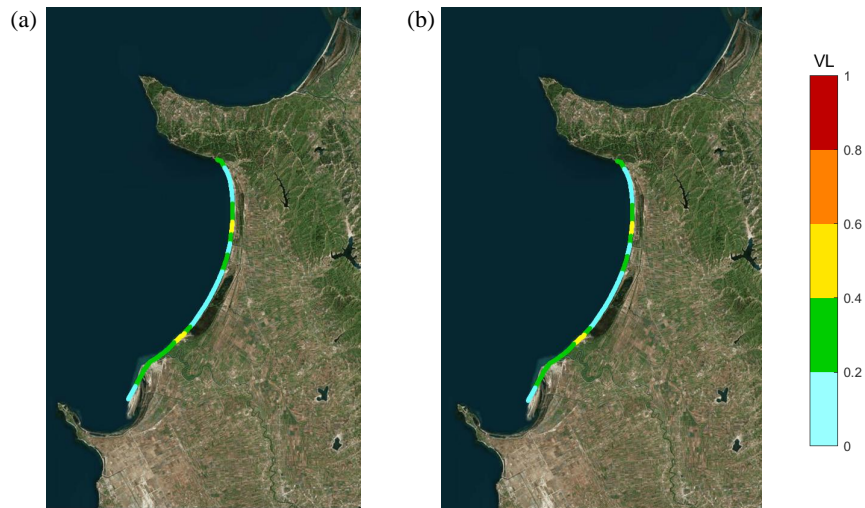


**Figure 9.** Run-up vulnerability levels for the Lalzit bay, using near-shore data for the 270-360°N sector: a) 50yr return period; b) 500yr return period

The directional analysis indicates that results are less varying with respect to the return period: if we refer to the 1<sup>st</sup> directional sector (180-270°N), 50yr return period, vulnerability levels are “very low” for all sections but 7 and 8, which show “low” vulnerability, and 0 (“medium vulnerability”). Switching to the 500yr return period, vulnerability rises from “very low” to “low” in sections -3, -1 and from “low” to “medium” in section 7, being unvaried in all the other ones. Results are slightly different for the 2<sup>nd</sup> (270-360°N) sector: in this case, 50yr vulnerability is “low” (instead of “very low”) for sections -3, -2, -1, 5, 11; section 7 shows a “medium” instead of a “low” vulnerability. Here, increasing the return period up to 500yr does not involve any variation in the resultants VL.

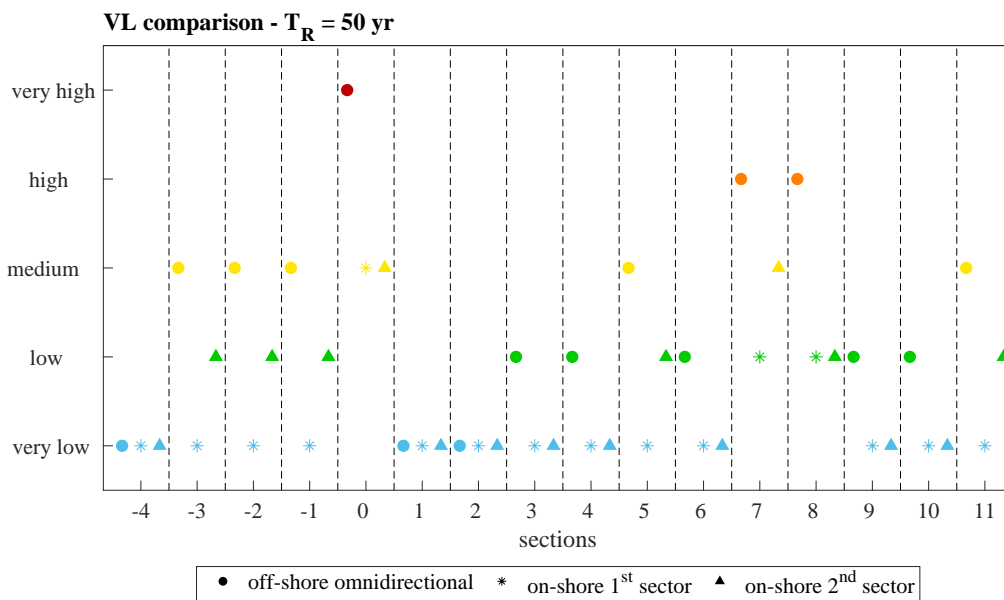


**Figure 10.** Comparison between the run-up vulnerability indexes for each sampling location; return period equal to 50yr

It is interesting to evaluate how VL can change due to the starting wave features: the extreme value analysis performed using deep-water data yields higher vulnerability levels than those obtained after propagating waves toward the shore. Referring to 50yr return period, the most exposed sections are yet characterized by “very high” (0) and “high” (7, 8) levels of vulnerability, whereas through the directional analysis vulnerability levels never happen to be higher than “medium”, despite the considered return period; to increase from 50yr to 500yr involve at most to move from a “low” to one step higher vulnerability level (section 7, 1<sup>st</sup> sector), precisely.

Actually, results divergence decreases for sections characterized by a “very low” vulnerability level in the northern part of the bay: in this case, the morphology of the surrounding beach seems to guarantee safe conditions, regardless to the magnitude of the forcing waves.

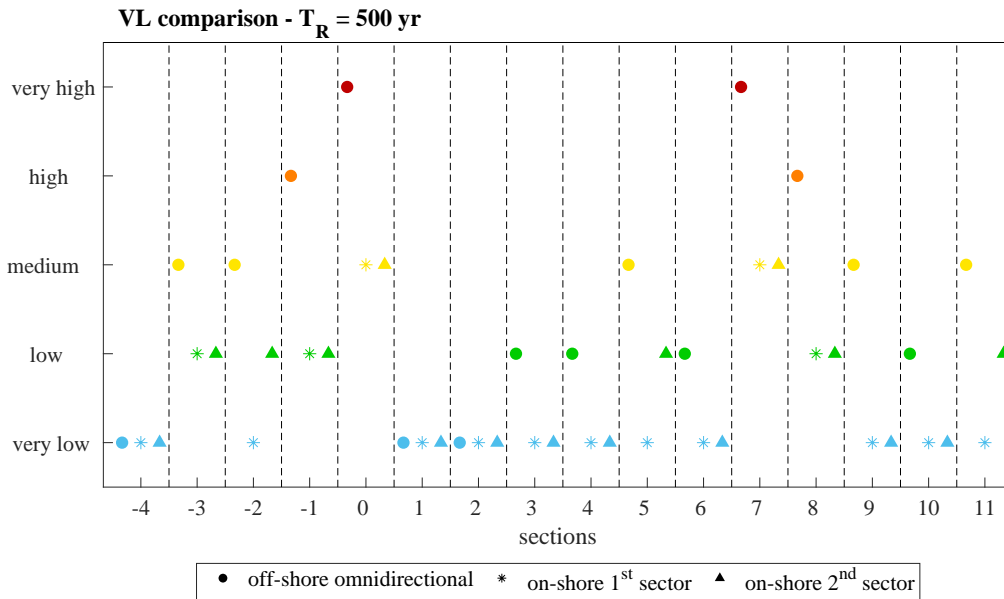


**Figure 11.** Comparison between the run-up vulnerability indexes for each sampling location; return period equal to 500yr

#### 4 Discussion

As a general trend, assessing coastal vulnerability to inundation using the wave climate computed at the local scale leads to lower vulnerability levels compared to those obtained through the regional analysis. If the vulnerability levels are similarly distributed along the bay (depending on the single section profiles), the long term run-up estimates are clearly dependent to the referring spatial scale: the geometry of the bay indeed strongly affects the waves' propagation toward the coast. Moving onshore, wave heights likely decrease due to refraction and diffraction, which can be expected to be the dominant processes as suggested by the concave enclosed shape of the coast. Consequently, run-up estimates come to be lower when dealing with the local-scale analysis, and resulting VL behave accordingly. It is worth mentioning that, as a common practice, this kind of computation is performed the other way round. Literally, when shallow water waves data are available, it is possible to propagate them backward through simple formulations in order to get the equivalent deep-water data to feed the run-up model with (like the Snell's law, see as an instance CERC, 1984). In this case, though, we did not propagate waves backward: we already had the off-shore data, furthermore the goal of the research is exactly to evaluate how VL change when employing shallow water parameters for estimating run-ups. Results reported in Fig. 10 and 11 highlight another important aspect: if we refer to the local scale, the vulnerability of the bay as a whole is higher when looking at the wave climate generally characterizing the 270-360°N sector. This outcome is justified as well by the geometry of the bay, in fact, even if the starting wave features representatives of the third quadrant are higher (Table 2), waves coming from W-NW are not diffracted by the southern cape as it happens instead for those coming from S-SW. The absence of obstacles along the waves path (but that of

the submerged bar) implies a lower reduction of the wave heights, involving in turn higher values of the following run-up, thus higher values for the IV variables. Nevertheless, differences between the long term wave parameters due to the considered return period are less pronounced than those of the 1<sup>st</sup> sector. This is still reflecting on the final run-up values, showing a lower variability which consequently reflects in the final vulnerability levels (whose values do not change among the considered return periods, as it happens instead when looking at the 180-270°N sector).

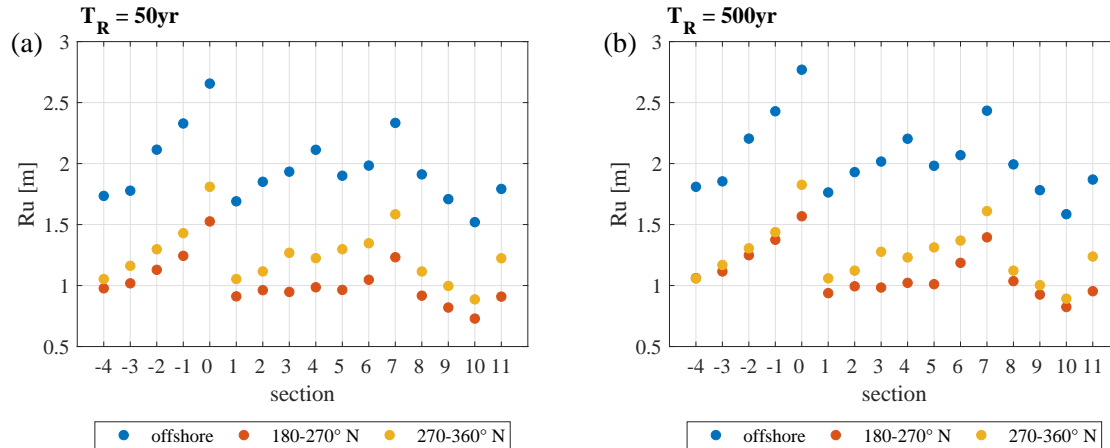


**Figure 12.** Comparison between run-up values for each section obtained through offshore (regional scale) and near-shore (local scale) conditions: a) 50yr return period; b) 500yr return period

Higher run-up estimates due to offshore analysis suggest another consideration about the different variability of the results between regional (offshore) and local (onshore) analysis: as previously demonstrated, the directional data result in a more homogeneous vulnerability level along the coastline. This can be simply justified looking at the vulnerability level computation: the same IV index may belong to different vulnerability classes, depending on the value that the  $IV_{max}$  variable gets; in fact, while  $IV_{min}$  is constant for any of the investigation approaches, the maximum IV depends on the run-up values (see Eq. (2)). High run-up imply lower  $IV_{max}$  values, thus a lower total range, which, being spaced in five classes anyway, leads to narrower intervals. Resulting vulnerability levels are therefore more sensitive to smaller variations of the IV values (as Fig. 10 and 11 show).

Finally, if we enlarge our analysis to the coastline as a whole, we can better appreciate how vulnerability is distributed. Despite the differences due to the referring wave data, the most vulnerable areas happen to be those nearby the Erzeni outflow and, in the north, towards the Rodoni cape (see Fig. 3a for references), even if for different causes. If we look at the berm height component, it is evident how the aforementioned areas are characterized by lower berms (Fig. 3d): the Erzeni outflow area has shown in the last years a significant ongoing coastal erosion, as it is estimated that the coastline is retreating at a speed of  $0.3 \div 0.5 \text{ m/y}$  (Boçi, 1994), resulting in the berms levelling; actually, the concurring reduction of the river sediment transport has also implied steeper profiles (Fig. 3c), that lead to higher run-up estimates. Moving to the north, the lower berms

are due instead to the anthropic activities recently developed, which required the levelling of the beach as well; concerning the cross-shore slope, there is actually no evidence of steeper profiles but that of section 7.

## 5 Summary and Conclusions

The vulnerability assessment of a coastline can be a helpful device to plan its land use, as an instance not considering to place high value activities when there's a high risk for the beaches of being submerged or eroded. In this framework, VL estimates provide an easy and reliable tool, in order to get an overall overview about a shore vulnerability distribution toward either inundation and/or erosion events.

In this paper, we evaluated the coastal inundation vulnerability for the bay of Lalzit (Durrës, Albania), following the model proposed by Bosom and Jiménez (2011). We first performed a regional analysis, referring to the original formula of Stockdon et al. (2006) in order to compute the extreme values for the run-ups at sixteen sections along the bay; then, we detailed the study downscaling the wave features in the shallow waters thanks to a wave propagation model.

We showed that, even if the vulnerability distribution do not change along the shore (e.g. the most exposed sections are placed in the same areas), the results linked to the local scale yield considerably lower vulnerability levels. This is mainly due to the run-up estimates, which are very sensitive to the input wave characteristics, which may be defined in shallow or deep waters. In the case of Lalzit, when waves propagation processes (such as refraction and breaking) become influential, run-up estimates can considerably change depending on the level of detail of wave characterization, as vulnerability levels accordingly do.

Since S2006 returns a high statistic for the run-up variable, it appears more plausible to refer to the modified model as proposed by Sancho-García et al. (2012), to estimate the return period linked to a closer run-up *expected value*. This precaution may allow to get more representative VL assessment, properly scaling their related values due to the chosen return period, particularly when the modifying processes of the waves are relevant. A critical analysis of the coastline vulnerability could prevent to adopt too much conservative approaches, that could lead to unnecessary countermeasures, translating to loss of money and invasive non required interventions.

The feasibility of VL assessment can represent a crucial ingredient for rapidly developing and transforming coastal regions such as the Lalzit bay in Albania, which present more options to drive virtuous future coastal development compared to industrialized countries, where coastal vulnerability assessment may mostly represent a tool for ICZM applied to manage conflicts among relevant stakeholders.

*Acknowledgements.* This study is part of a project shared between the University of Trento and the University of Genoa (Italy), along with the Polytechnic of Tirana (Albania). The authors would like to thank everyone who joined the field data collection: Alessandro Chesini, Alessandro Dotto, Alessio Maier, Daniele Spada, Dario Guirrieri, Erasmo Vella, Federica Pedon, Giorgio Gallerani, Laura Dalla Valle, Martina Costi, Navarro Ferronato, Stefano Gobbi, Tommaso Tosi (University of Trento), Ardit Omeri, Arsela Caka, Bardhe Gjini, Bestar Cekrezi, Erida Beqiri, Ferdinand Fufaj, Ildir Lami, Marie Shyti, Mikel Zhidro, Nelisa Haxhi, Xhon Kraja, Tania Floqi (Tirana Polytechnic). The col-



lected data were then analysed by the Italian partners, in the framework of the UNESCO Chair in Engineering for Human and Sustainable Development (DICAM-Unesco Chair). G. Besio has been funded by University of Genoa through “Fondi per l’Internazionalizzazione” grant.

## References

- Battjes, J. A.: Run-up distributions of waves breaking on slopes, *Journal of Waterways and Harbors Division*, 97, 91–114, 1971.
- Blott, S. J. and Pye, K.: GRADISTAT: a grain size distribution and statistics package for the analysis of unconsolidated sediments, *Earth surface processes and Landforms*, 26, 1237–1248, 2001.
- 5 Boçi, S.: Evoluzione e problematiche ambientali del litorale albanese, *Bollettino della Societa Geologica Italiana*, 113, 7–14, 1994.
- Booij, N., Ris, R., and Holthuijsen, L.: A third-generation wave model for coastal regions, *J. Geophys. Res.*, 104, C4, 2003.
- Bosom, G. E. and Jiménez, Q. J. A.: Probabilistic coastal vulnerability assessment to storms at regional scale: application to Catalan beaches (NW Mediterranean), *Natural hazards and Earth system sciences*, 11, 475–484, 2011.
- Callaghan, D., Nielsen, P., Short, A., and Ranasinghe, R.: Statistical simulation of wave climate and extreme beach erosion, *Coastal Engi-*  
10 *neering*, 55, 375–390, 2008.
- CERC: Shore Protection Manual, US Army Corps of Engineers, Washington, DC, 1984.
- Ciccarelli, D., Pinna, M., Alquini, F., Cogoni, D., Ruocco, M., Bacchetta, G., Sarti, G., and Fenu, G.: Development of a coastal dune vulnerability index for Mediterranean ecosystems: A useful tool for coastal managers?, *Estuarine, Coastal and Shelf Science*, 187, 84 – 95, 2017.
- 15 Claps, P. and Laio, F.: Can continuous streamflow data support flood frequency analysis? An alternative to the partial duration series approach, *Water Resources Research*, 39, 2003.
- Coles, S. and Pericchi, L.: Anticipating catastrophes through extreme value modelling, *Journal of the Royal Statistical Society: Series C (Applied Statistics)*, 52, 405–416, 2003.
- Coles, S., Bawa, J., Trenner, L., and Dorazio, P.: An introduction to statistical modeling of extreme values, vol. 208, Springer, 2001.
- 20 De Leo, F., Besio, G., Zolezzi, G., Bezzi, M., Floqi, T., and Lami, I.: Coastal erosion triggered by political and socio-economical abrupt changes: the case of Lalzit Bay, Albania, *Proc 35th International Coastal Engineering Conference, ASCE*, 1, 13, 2017.
- Di Paola, G., Aucelli, P. P. C., Benassai, G., and Rodríguez, G.: Coastal vulnerability to wave storms of Sele littoral plain (southern Italy), *Natural hazards*, 71, 1795–1819, 2014.
- Di Risio, M., Bruschi, A., Lisi, I., Pesarino, V., and Pasquali, D.: Comparative Analysis of Coastal Flooding Vulnerability and Hazard  
25 *Assessment at National Scale*, *Journal of Marine Science and Engineering*, 5, 2017.
- Ferreira, O., Plomaritis, T. A., and Costas, S.: Process-based indicators to assess storm induced coastal hazards, *Earth-Science Reviews*, 173, 159 – 167, 2017.
- Ferreira Silva, S., Martinho, M., Capitão, R., Reis, T., Fortes, C., and Ferreira, J.: An index-based method for coastal-flood risk assessment in low-lying areas (Costa de Caparica, Portugal), *Ocean and Coastal Management*, 114, 90–104, 2017.
- 30 Fitton, J. M., Hansom, J. D., and Rennie, A. F.: A national coastal erosion susceptibility model for Scotland, *Ocean and Coastal Management*, 132, 80 – 89, 2016.
- Forristall, G. Z.: On the use of directional wave criteria, *Journal of waterway, port, coastal, and ocean engineering*, 130, 272–275, 2004.
- Garrity, N. J., Battalio, R., Hawkes, P. J., and Roupe, D.: Evaluation of event and response approaches to estimate the 100-year coastal flood for Pacific coast sheltered waters, in: *30th International Conference on Coastal Engineering, ICCE 2006*, 3 September 2006 through 8  
35 *September 2006*, San Diego, CA, United States, pp. 1651–1663, 2007.
- Gornitz, V. M., Daniels, R. C., White, T. W., and Birdwell, K. R.: The development of a coastal risk assessment database: vulnerability to sea-level rise in the US Southeast, *Journal of Coastal Research*, pp. 327–338, 1994.

- Haver, S.: Wave climate off northern Norway, *Applied Ocean Research*, 7, 85–92, 1985.
- Hawkes, P. J., Gouldby, B. P., Tawn, J. A., and Owen, M. W.: The joint probability of waves and water levels in coastal engineering design, *Journal of hydraulic research*, 40, 241–251, 2002.
- Holman, R.: Extreme value statistics for wave run-up on a natural beach, *Coastal Engineering*, 9, 527–544, 1986.
- 5 Kamphuis, J. W.: Introduction to coastal engineering and management, vol. 30, World Scientific Publishing Co Inc, 2010.
- Lang, M., Ouarda, T., and Bobée, B.: Towards operational guidelines for over-threshold modeling, *Journal of hydrology*, 225, 103–117, 1999.
- Mase, H.: Random Wave Runup Height on Gentle Slope, *Journal of Waterway, Port, Coastal, and Ocean Engineering*, 115, 649–661, 1989.
- Massey Jr, F. J.: The Kolmogorov-Smirnov test for goodness of fit, *Journal of the American statistical Association*, 46, 68–78, 1951.
- Mathisen, J. and Bitner-Gregersen, E.: Joint distributions for significant wave height and wave zero-up-crossing period, *Applied Ocean*  
 10 *Research*, 12, 93–103, 1990.
- Mavromatidi, A., Briche, E., and Claeys, C.: Mapping and analyzing socio-environmental vulnerability to coastal hazards induced by climate change: An application to coastal Mediterranean cities in France, *Cities*, 72, 189 – 200, 2018.
- Mentaschi, L., Besio, G., Cassola, F., and Mazzino, A.: Developing and validating a forecast/hindcast system for the Mediterranean Sea, *Journal of Coastal Research*, SI 65, 1551–1556, 2013.
- 15 Mentaschi, L., Besio, G., Cassola, F., and Mazzino, A.: Performance evaluation of WavewatchIII in the Mediterranean Sea, *Ocean Modelling*, 90, 82–94, 2015.
- Montreuil, A.-L., Chen, M., and Elyahyoui, J.: Assessment of the impacts of storm events for developing an erosion index, *Regional Studies in Marine Science*, 16, 124 – 130, 2017.
- Narra, P., Coelho, C., Sancho, F., and Palalane, J.: CERA: An open-source tool for coastal erosion risk assessment, *Ocean and Coastal*  
 20 *Management*, 142, 1 – 14, 2017.
- Neumann, B., Vafeidis, A. T., Zimmermann, J., and Nicholls, R. J.: Future coastal population growth and exposure to sea-level rise and coastal flooding-a global assessment, *PloS one*, 10, e0118 571, 2015.
- Plant, N. G. and Stockdon, H. F.: How well can wave runup be predicted? Comment on Laudier et al.(2011) and Stockdon et al.(2006), *Coastal Engineering*, 102, 44–48, 2015.
- 25 Sancho-García, A., Guillén, J., Simarro, G., Medina, R., and Cánovas, V.: Beach inundation prediction during storms using different wave heights as inputs, *Proc 33th International Coastal Engineering Conference, ASCE*, 1, 32, 2012.
- Satta, A., Snoussi, M., Puddu, M., Flayou, L., and Hout, R.: An index-based method to assess risks of climate-related hazards in coastal zones: The case of Tetouan, *Estuarine, Coastal and Shelf Science*, 175, 93–105, 2016.
- Soukissian, T. H., Ntoumas, M. C., Anagnostou, C., Kiriakidou, C., et al.: Coastal Vulnerability of Eastern Saronikos Gulf to intense natural  
 30 events, in: *The Twentieth International Offshore and Polar Engineering Conference, International Society of Offshore and Polar Engineers*, 2010.
- Stockdon, H., Holman, R., Howd, P., and Sallenger Jr., A.: Empirical parameterization of setup, swash, and runup, *Coastal Engineering*, 53, 573–588, 2006.
- UNEP, M.: ICZM Protocol in the Mediterranean, available at: [www.pap-thecoastcentre.org](http://www.pap-thecoastcentre.org), 2008.
- 35 Vitousek, S., Fletcher, C. H., and Barbee, M. M.: A practical approach to mapping extreme wave inundation: Consequences of sea-level rise and coastal erosion, in: *Solutions to Coastal Disasters 2008*, pp. 85–96, 2008.
- Wentworth, C. K.: A scale of grade and class terms for clastic sediments, *The Journal of Geology*, 30, 377–392, 1922.